

Longitudinal characterization of function and structure of Bietti crystalline dystrophy: report on a novel homozygous mutation in *CYP4V2*.

Catherine M. Lockhart, Travis B. Smith, Paul Yang, Malinu Naidu, Allan E. Rettie, Abhinav Nath, Richard G. Weleber, Edward J. Kelly

SUPPLEMENTARY MATERIALS

Supplementary Table S1. Primer sequences for PCR amplification and sequencing of *CYP4V2* DNA extracted from buccal swabs.

Supplementary Figure S1. Full-field ERGs of patient with Bietti Crystalline Dystrophy from 27.7 to 44.5 years of age.

Supplementary Table S2. Normal values for full-field ERG and values for the patient with Bietti Crystalline Dystrophy.

Supplementary Figure S2. Analysis of full-field ERG components as correlates of age and Indicators of progression.

Supplementary Table S3. Linear and Quadratic Equations, RMSE, and R^2 for curve fitting presented in Supplementary Figure S2.

Supplementary Figure S3. Analysis of visual field volumetric indices, V_{tot} and V_{30° , with Age, Eye, and the Event.

Supplementary Appendix. Analysis of static visual field progression and modeling of the hill of vision and its longitudinal changes.

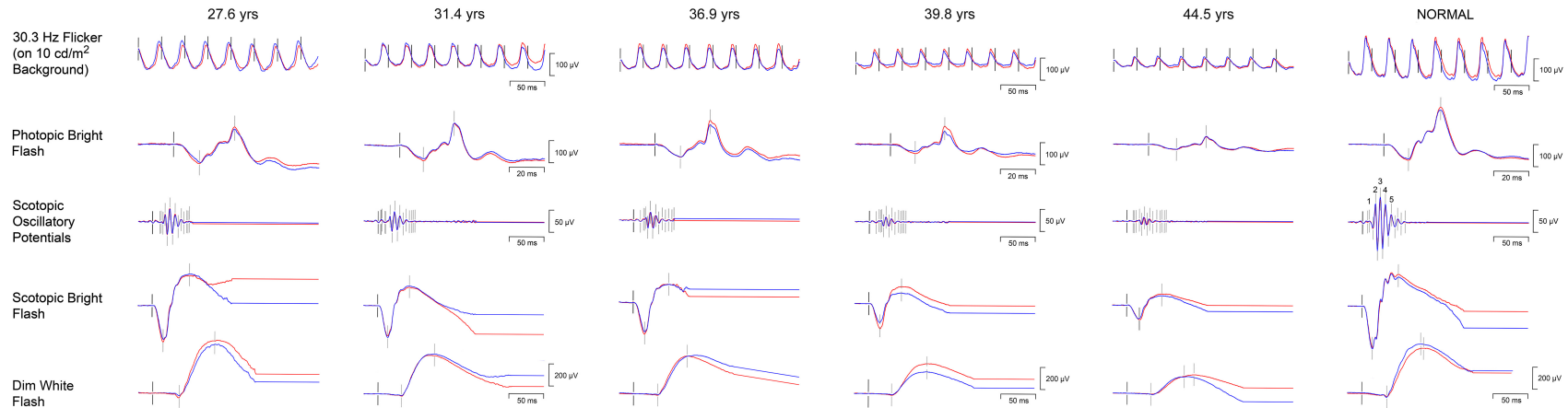
References for Supplementary Appendix.

Supplementary Table S1. Primer sequences for PCR amplification and sequencing of CYP4V2 DNA extracted from buccal swabs.

Exon	Amplification		Sequencing	
	Forward Primer	Reverse Primer	Forward Primer	Reverse Primer
1	5'ACGGGTAGCTGACTTCCTA3'	5'CATTCTCCACAGGGTGACAGG3'	5'CCCAAAGCCTCCCTGGATTA3'	5'GGGTTCCCTGGCTGATCGGAG3'
2	5'CTACCTGGCTTCCTCTAACAG3'	5'TTTTTGTGCTGAAATGGCTGAA3'	5'GAATTAGTATATTCATCAA3'	5'ATATAAGGACACGTTATATT3'
3	5'AGATTGCGCTCCTCCCACTCAC3'	5'ACCTGGACTCTTGGCCTCTGACG3'	5'CTAGCTGTATTCTAGCCAGTA3'	5'GCCAGCTGCCAGGGACCT3'
4	5'TGCCAAAAGCATTGAGAACCTGT3'	5'CGCGCTGAAGAGCCCGTCA3'	5'GAAGCTGTTTCAGGAGAA3'	5'CCGTACCCCTTTCCGTCCC3'
5	5'AGGAAGAAGCAGGAACAGGGAGTAG3'	5'CAACGCAGAAATTGTTAGCAATAA3'	5'GACAAAGCAGGATGTACGTC3'	5'GCAATAATTTTAAAGCCTA3'
6	5'GCTTCATGGGATGCGTGGT3'	5'GAAATGAACGGTGGGGATGGT3'	5'CCCACGATTGCCTTCAACAAG3'	5'GCACAACATCGTGAAATGAC3'
7	5'GAGCCTATGTTGTCGAAATGT3'	5'TCTGAAGAAGTTGAGCTGTACTT3'	5'AGAACTAGCATATTTTATA3'	5'CTTCTTTAGTTAACTACTT3'
8	5'GTTTGCAGTCACAGTGCAGTC3'	5'CCAGCATCCGGCCTAGTACAGTC3'	5'AATCCAGAGACAATCAA3'	5'GTGACATCTCTGCAGACT3'
9 & 10	5'ATGCCATGCCTTGATCCACCTGT3'	5'TGGGCAATGTCACATCACATCTCA3'	5'TTAGATGTCTGCACCACCAG3'	5'AAATCACTGTGAGAACCA3'
11	5'CTCTTCATCTTTAACAGGTGTTCC3'	5'CAAACTCAAACTTTTTCTTTGT3'	5'AGCCATTCTGGTTCTCTTC3'	5'TCAAGATCAGTGGGATCAAG3'

After 5 minutes at 94°C, the annealing phase consisted of ten cycles with 15 sec at 94°C, 30 sec at 65°C decreasing 1°C per cycle, and 60 sec at 72°C, then the amplification phase consisted of 30 cycles with 15 sec at 94°C, 30 sec at 55°C, and 60 sec at 72°C. For each reaction, 1 µL of sample DNA was added to a mixture containing 0.25 µL DMSO (Sigma-Aldrich, St. Louis, MO, USA), 5.2 µL 5M betaine (Sigma-Aldrich), 0.25 µL GemTaq™ DNA polymerase (MGQuest, Lynnwood, WA, USA), 4.0 µL GemTaq™ buffer in 1.5 mM MgCl₂ (MGQuest, Lynnwood, WA, USA), 200 µM dNTPs (Qiagen, Valencia, CA, USA), 300 µM each amplification forward and reverse primer (Integrated Data Technologies, San Diego, CA, USA), and nanopure water to a final volume of 20 µL. The **Supplemental Table S1** lists the forward and reverse primer sequences used for each reaction. Correct PCR amplification was validated by gel electrophoresis using 1.5% agarose gel, and amplicons were isolated using a QIAquick® PCR Purification Kit following the manufacturer protocol (Qiagen, Valencia, CA, USA). Sequencing reactions containing 0.5 µL sequencing primer for either forward or reverse reactions (Integrated Data Technologies, San Diego, CA, USA), 5 µL of isolated amplicons, and 4.5 µL of nanopure water were prepared and submitted for sequencing by Operon (Eurofins Genomics, Huntsville AL, USA). Sequencing results were analyzed for homology to known CYP4V2 sequence using the Basic Local Alignment Search Tool (BLAST, <http://blast.ncbi.nlm.nih.gov>).

Supplementary Figure S1. Full-field ERGs of patient with Bietti Crystalline Dystrophy from 27.7 to 44.5 years of age.



The above illustration depicts the tracings for the full-field ERGs as performed on the patient at 5 time points, beginning at the initial time the patient was seen by one of the authors (RGW). The ERG methodology and protocol have been previously reported^{1,2,3} and conform to ISCEV standard.⁴ The age of the patient at each test is designated above the column. The rows show the 5 major components of the ISCEV (from top to bottom): 30.3 Hz Flicker (on a 10 cm/m² background), Photopic Bright Flash, Scotopic Oscillatory Potentials, Scotopic Bright Flash, and Scotopic Dim White Flash. The last column shows the responses of a normal subject of similar age to the patient at her last ERG. For each ERG component, the tracing in red is the average of multiple tracings for the right eye and the tracing in blue is the average of multiple tracings from the left eye. The black vertical bar indicates the stimulus occurrence. The peak of the positive b-wave response is designated by a faint vertical line on the tracing. The calibration scale for amplitude is in unit microvolt (μV) and the implicit time is in unit millisecond (ms). Preamplifier bandpass was 0.1 - 1000 Hz for the single flash and Flicker response. The Scotopic Oscillatory Potentials were extracted by digital filtration (bandpass 100-300 Hz) from the Scotopic Bright Flash responses. The Oscillatory Potential Peaks were ordered as previously described² and as shown for the normal ERG in the last column. The Scotopic Oscillatory Wavelet Index was calculated by summation of amplitudes of peaks 2 through 5. The Photopic Negative Response (PhNR)^{5,6} is a recently defined component of the Photopic Bright flash response that follows the b-wave and, when present, the i-wave, as a negative-going wave with its nadir about 65 ms after stimulus occurrence. The PhNR reflects the electrical activity of the retinal ganglion cells and is abnormal in glaucoma and in retinal diseases that affect the inner retinal elements.

Supplementary Table S2. Normal values for full-field ERG and values for the patient with Bietti Crystalline Dystrophy.

		Dim White Flash b-wave		Scotopic Bright Flash a-wave		Scotopic Bright Flash b-wave		Scotopic BF OP Wavelet Index	Photopic Bright Flash a-wave		Photopic Bright Flash b-wave		Photopic Negative Response		30.3 Hz Flicker (10 cd/m ²)	
		Amp	Imp Time	Amp	Imp Time	Amp	Imp Time	Amp	Amp	Imp Time	Amp	Imp Time	Amp	Imp Time	Amp	Imp Time
Normal Mean (± SD)		442 ± 80.1	86.0 ± 6.7	357 ± 64.1	15.1 ± 0.71	620 ± 128	51.4 ± 4.1	186 ± 77.4	63.2 ± 13.0	13.6 ± 0.74	221 ± 50.7	30.7 ± 1.6	64.4 ± 21.1	63.6 ± 3.0	130 ± 28.8	24.8 ± 2.1
Upper 95% CI		599	99.1	483	16.5	871	59.4	338	88.7	15.1	320	33.8	113	69.5	186	28.9
Lower 95% CI		285	72.9	231	3.7	369	43.4	34.3	37.7	12.1	121	27.1	23.0	58.5	73.6	20.7
ERG 27.6 yrs	OD	512	87.0	303	16.0	598	53.0	133	80.0	14.6	150	34.6	84.6	67.6	119	29.3
	OS	475	68.5	341	16.0	611	51.0	145	78.2	15.4	136	34.4	102	67.2	101	30.3
ERG 31.4 yrs	OD	373	80.0	283	14.5	464	45.0	98.7	62.6	13.4	154	30.8	64.7	63.8	93.0	25.6
	OS	366	72.5	270	14.5	437	45.0	95.7	54.4	14.0	147	31.0	57.7	65.0	90.2	25.9
ERG 36.9 yrs	OD	354	76.0	278	16.5	455	50.5	71.4	53.4	14.4	164	31.2	48.2	65.0	103	27.9
	OS	354	86.5	256	16.5	438	51.0	80.4	49.2	14.6	145	31.2	66.9	61.8	88.4	28.1
ERG 39.7 yrs	OD	288	84.5	225	16.0	379	46.5	44.4	39.5	14.0	124	30.8	54.4	65.2	75.7	26.8
	OS	207	83.0	170	16.0	268	44.0	43.5	28.9	13.4	93.1	30.8	41.5	64.6	54.5	26.3
ERG 44.4 yrs	OD	178	95.0	128	19.0	232	50.0	36.1	22.1	15.6	57.7	32.6	28.5	66.0	40.0	30.8
	OS	178	85.5	122	17.0	208	49.5	34.9	20.8	15.2	58.7	32.8	29.6	66.4	43.3	29.8

The amplitudes and implicit times for the averaged right and left eye ffERG components in a cohort of 10 normal subjects (mean age 40, range 19-49 yrs) are presented in **Supplementary Table 2**. The values for the Upper and Lower 95% confidence interval (CI) were calculated as the mean ± 1.96 SD. The ffERG amplitudes and implicit times are presented for each eye of the patient with Bietti

crystalline dystrophy at each of the 5 test sessions depicted in **Figure S1**. The value for the amplitude and implicit time at the time when it first fell outside the 95% CI are emboldened and red. The implicit times were mostly normal, with mild delays in the later studies. The amplitudes were initially within the normal range for the first ERG for all components and over the nearly 17 years of follow-up, slowly declined. The rod b-wave amplitude (Dim White Flash) was 116% of normal mean OD and 107% of normal mean OS at 27.6 years of age, first became subnormal (at 47% of mean) for the left eye at age 39.7 and was even lower (40% of normal mean) at age 44.4 years. The rod b-wave implicit times remained within the upper range of normal. The a-wave and b-wave amplitudes for the mixed rod-cone Scotopic Bright Flash and the Photopic Bright Flash became mildly to moderately subnormal for amplitude for each eye, more so from the left eye, by 39 years of age, continued to decline, and were markedly subnormal (~25-35% of normal amplitude) at 44 years of age. The different component amplitudes appeared to be variably affected over time. The cone Photopic Bright Flash b-wave was 68%OD and 62% OS of the normal mean at age 27 yrs and decreased to ~26% of normal at age 44 yrs. The 30.3 Hz Flicker amplitude was 92% OD, 78% OS of normal at age 27.6 and ~32% of normal at age 44.4 yrs. The Photopic BF a-wave and b-wave implicit times were, at times, minimally delayed but mostly remained near the high end of normal.

The amplitudes of the Scotopic OP Wavelet Index and the PhNR, in our experience, vary over a large range in normal subjects. This produces a greater mean and a larger SD, which leads to a wider 95% confidence interval that can impede or delay the determination of statistically significance progression. In these instances, change in the percentage of each test session compared to the normal mean could be followed in addition to absolute microvolt levels.

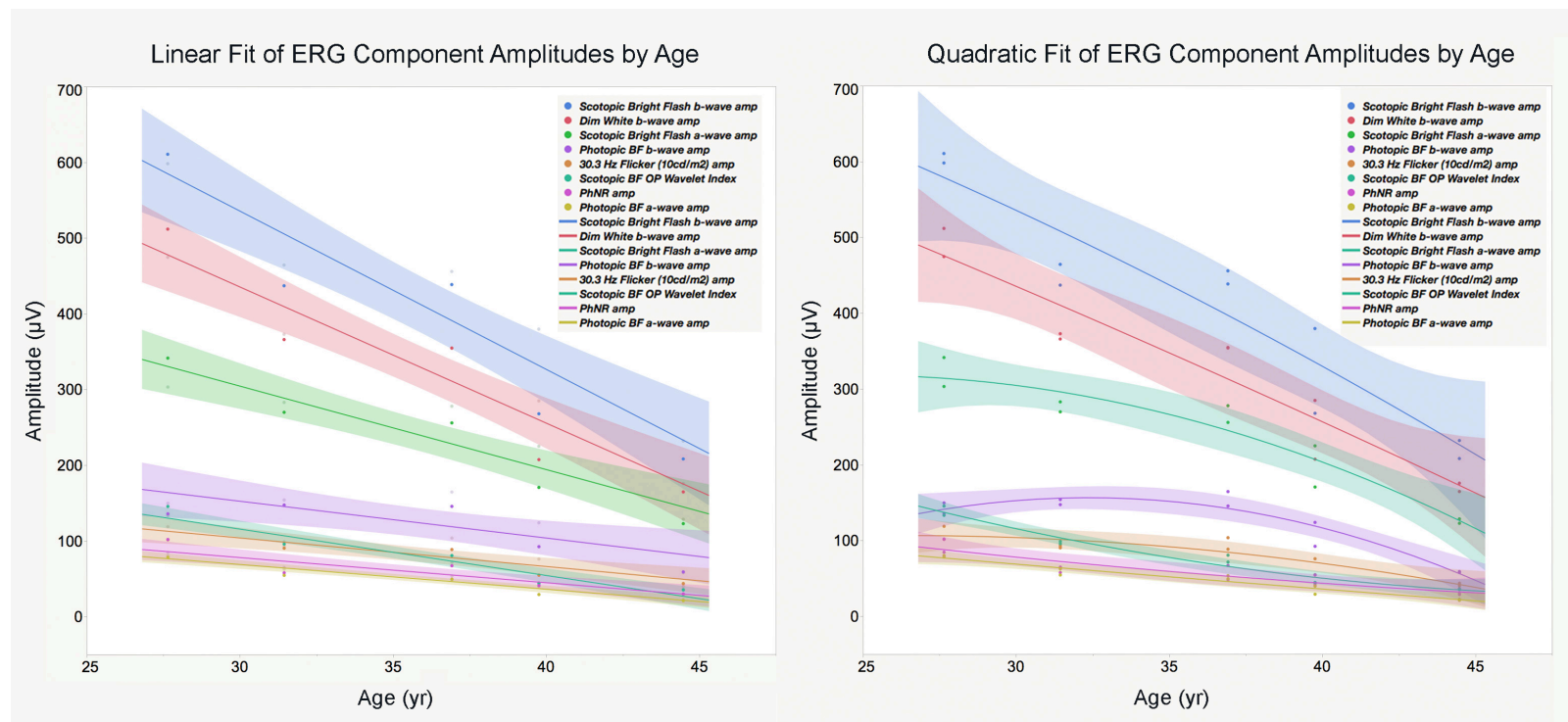
The Scotopic OP Wavelet Index for the patient with Bietti crystalline dystrophy at age 27.6 yrs was 71-78% of normal. At age 44.4 yrs, it had decreased to ~19% of normal but was still not below the lower 95% CI of 34.3 μ V. Similarly, the PhNR amplitude was 131% of normal OD and 158% of normal OS at age 27.6 yrs and decreased to 44-46% of normal mean at age 44.1 yrs, but has not yet dropped below the lower limit of normal, 23 μ V.

Analysis of components of the full-field ERG, as correlates of age and Indicators of progression.

The modeling platform in JMP 12 (Carey, NC: SAS Institute, Inc.) was used to screen and assess linear relationships between the dependent variables, amplitude and implicit time, for each component of the ffERG, and the independent variables age and eye. The screening report returns terms that evaluate significance associations of any of multiple dependent variables with the independent variables. An individual p-value is produced that is analogous to the standard p-value for a linear model, for each of the dependent variables for each independent variable, with a small value indicating a significant effect. We considered as significant a p-value of ≤ 0.05 . The platform also reports the simultaneous p-value, which is similar to the individual p-value, but multiple-comparison adjusted. ANOVA was used to further assess significance and almost invariably revealed no significance linear effect when the individual p-value and simultaneous p-value were both insignificant. In Instances where the individual p-value was clearly significant but the simultaneous p-value was not, most often ANOVA found either no significance or, in some instances, a lower level of significance with a mixture of linear and more complex interactions. A p-value of $\leq .05$ was considered significant.

For none of the ffERG component amplitudes or implicit times was there an effector relationship detected for the independent variable Eye. For the implicit times of the ffERG components, the screening model followed by ANOVA found no significant correlation with Age of the patient. Significant individual and simultaneous p-values were, however, obtained on screening Age with 8 dependent amplitude variables of the components of the ffERG. ANOVA confirmed significance for these variable at the p-values designated in parentheses for Age and constructed predictive equations for 1) Scotopic Bright Flash b-wave ($p < .0001$), 2) Dim White b-wave amplitude ($p < .0001$), 3) Scotopic Bright Flash a-wave ($p < .0001$), 4) Photopic b-wave amplitude ($p = .0003$), 5) Scotopic Bright Flash Oscillatory Wavelet Index ($p < .0001$), 6) 30.3 Hz Flicker amplitude, ($p < .0001$), 7) PhNR amplitude ($p = .0003$), and 8) Photopic a-wave amplitude ($p < .0001$). The amplitude dependent variable that showed significant age effects were graphed first to a linear fit followed by a quadratic fit as shown below. In almost all instances, the curve fitting program replicated the predictive linear equation created by the ANOVA.

Supplementary Figure S2. Analysis of full-field ERG component amplitudes as correlates of age and indicators of progression



Supplementary Table S3. Linear (Left) and Quadratic (Right) Equations, RMSE, and R² for Supplementary Figure S2

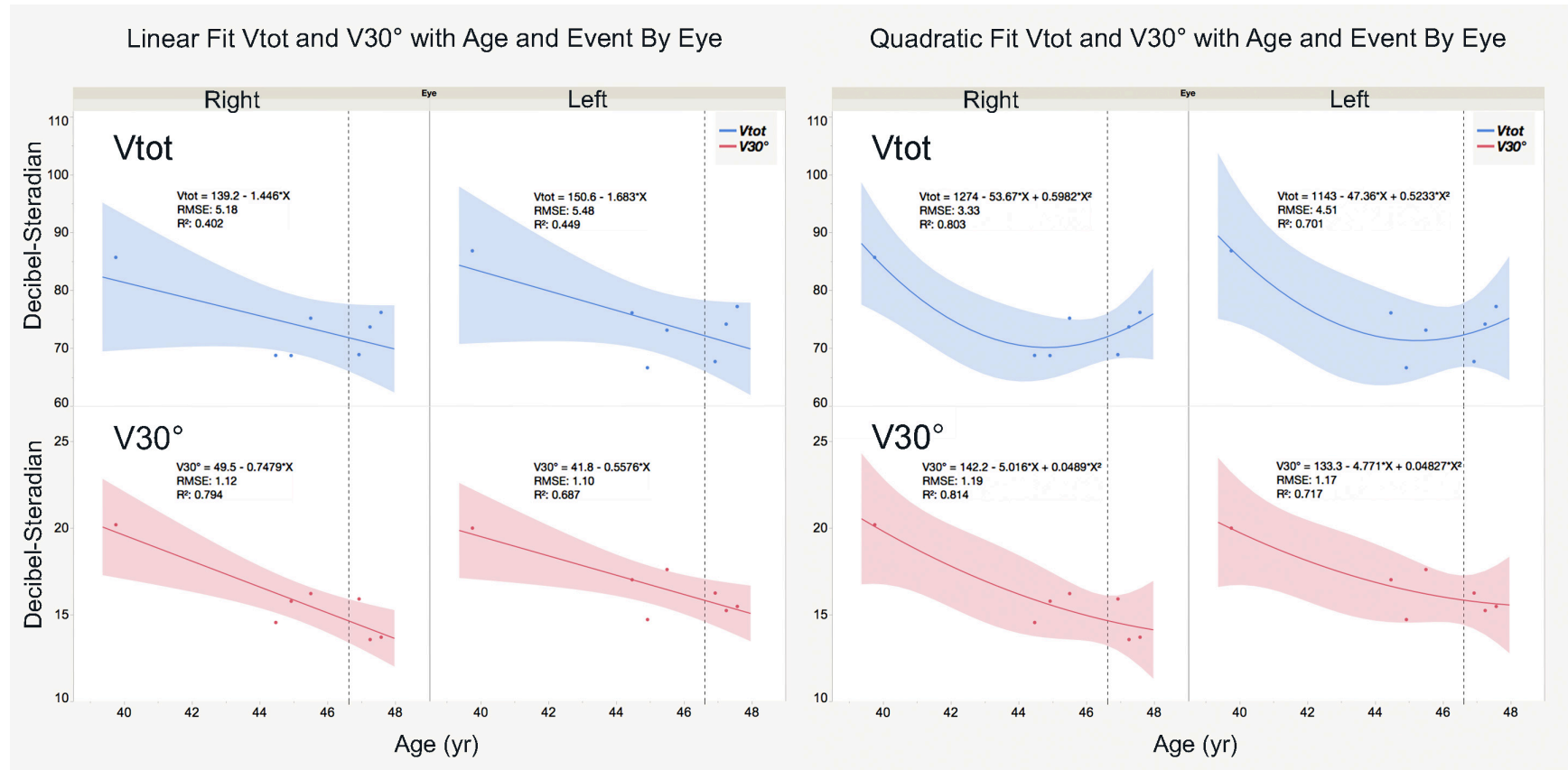
Scotopic Bright Flash b-wave amp = 1163 - 20.92*Age RMSE(Scotopic Bright Flash b-wave amp) = 53.83 R ² (Scotopic Bright Flash b-wave amp) = 0.88	Scotopic Bright Flash b-wave amp = 940.8 - 8.19*Age - 0.1772*Age ² RMSE(Scotopic Bright Flash b-wave amp) = 53.97 R ² (Scotopic Bright Flash b-wave amp) = 0.88
Dim White Flash b-wave amp = 975.3 - 18*Age RMSE(Scotopic Bright Flash b-wave amp) = 38.18 R ² (Dim White Flash b-wave amp) = 0.91	Dim White Flash b-wave amp = 898.3 - 13.59*Age + 0.06132* Age ² RMSE(Scotopic Bright Flash b-wave amp) = 40.79 R ² (Dim White Flash b-wave amp) = 0.91
Scotopic Bright Flash a-wave amp = 635.7 - 11.04*Age RMSE(Scotopic Bright Flash a-wave amp) = 28.96 R ² (Scotopic Bright Flash a-wave amp) = 0.61	Scotopic Bright Flash a-wave amp = 15.56 + 24.45*Age - 0.4938* Age ² RMSE(Scotopic Bright Flash a-wave amp) = 25.58 R ² (Scotopic Bright Flash a-wave amp) = 0.91
Photopic Bright Flash b-wave amp = 298.9 - 4.884*Age RMSE(Scotopic Bright Flash b-wave amp) = 26.24 R ² (Scotopic Bright Flash b-wave amp) = 0.90	Photopic Bright Flash b-wave amp = - 559 + 44.22*Age - 0.6832* Age ² RMSE(Scotopic Bright Flash b-wave amp) = 14.30 R ² (Scotopic Bright Flash b-wave amp) = 0.90
30.3 Hz Flicker (10cd/m ²) amp = 217.2 - 3.782*Age RMSE (30.3 Hz Flicker (10cd/m ²) amp): = 13.16 R ² ((30.3 Hz Flicker (10cd/m ²)) = 0.79	30.3 Hz Flicker (10cd/m ²) amp = -28.57 + 10.28*Age - 0.1957* Age ² RMSE (30.3 Hz Flicker (10cd/m ²) amp): = 12.26 R ² ((30.3 Hz Flicker (10cd/m ²)) = 0.84
Scotopic BF OP Wavelet Index = 299.9 - 6.145*Age RMSE (Scotopic BF OP Wavelet Index) amp): = 10.72 R ² ((Scotopic BF OP Wavelet Index) = 0.94	Scotopic BF OP Wavelet Index = 567.4 - 21.45*Age + 0.213* Age ² RMSE (Scotopic BF OP Wavelet Index) amp): = 8.64 R ² ((Scotopic BF OP Wavelet Index) = 0.96
Photopic Negative Response (PhHR) = 178.3 - 3.344*Age RMSE (Photopic Negative Response (PhHR)) amp): = 10.38 R ² (Photopic Negative Response (PhHR)) = 0.82	Photopic Negative Response (PhHR) = - 7.695*Age + 0.06054* Age ² RMSE (Photopic Negative Response (PhHR)) amp): = 10.89 R ² (Photopic Negative Response (PhHR)) = 0.84
Photopic Bright Flash a-wave amp = 167.1 - 3.245*Age RMSE(Scotopic Bright Flash a-wave amp) = 5.51 R ² (Scotopic Bright Flash a-wave amp) = 0.94	Photopic Bright Flash a-wave amp = 1881.2 - 4.086*Age + 0.01125* Age ² RMSE(Scotopic Bright Flash a-wave amp) = 5.88 R ² (Scotopic Bright Flash a-wave amp) = 0.94

The graphs above depict the linear fit (Left) and quadratic fit (Right) of the ERG component amplitude data with age. Supplementary Table S3 presents the equations and the parameters of the fit. The root mean square error (RMSE) assessed the variance and R^2 , the overall goodness of the fit. The equation for the linear fit of the ERG components amplitudes against age were identical to the equation derived from ANOVA. RMSE and R^2 were similar for the linear and quadratic fit for the dependent amplitude variables for Scotopic Bright Flash b-wave, Dim White b-wave, and PhNR, suggesting that quadratic curve fitting, compared to linear regression, would not reveal additional insights into the mathematical relationships of these data. For the amplitude variables for the Scotopic Bright Flash a-wave, Photopic Bright Flash a-wave, 30.3 Hz flicker, and Scotopic Bright Flash Oscillatory Wavelet Index, the RMSE was lower and/or the R^2 was higher, indicating lower variance and/or better overall fit of the data with the quadratic fit. This opened the possibility that for these components, the quadratic equation may reveal additional insight into the nature of the disease.

The interpretation of a better fit of data with a quadratic or non-linear equation compared to a simple linear regression is difficult. A quadratic fit will always appear to fit better because the model is less parsimonious. Processes can occur in both disease where linear regression may not fit the data well. A recent paper⁷ reported that the distribution of volumetric visual field indices for a cohort of normal subjects,⁸ was fit better with a quadratic than a linear equation. Gardiner et al.⁹ reported that a better fit of progression in glaucoma can be achieved for certain indices through use of non-linear curve fitting, including piecewise linear regression, and even recommended comparisons of patient data with the normal hill of vision in order to achieve a better appreciation of the complexities unique to each patient. Although this article was written in the context of glaucoma, many of the points made by Gardiner and his colleagues have direct relevance to modeling progression of loss of structure and function in inherited retinal degeneration. Extensive, multi-cellular, structural, neurophysiologic, and functional adaptive remodeling occurs in the retina following deafferentation from loss of photoreceptors. Retinal remodeling can produce multiple changes, many of which may reside in inner retinal layers, that could influence the rate and nature of progression or enact differing rates of progression in different regions of the retina.¹⁰ Retinal remodeling introduces complex noise that interferes with retinal functioning and offers possible explanations for why progression in chronic diseases, such as inherited retinal degenerations, might be better fit by non-linear models.

Static visual fields were first performed for the patient at age 39.8 yrs of age and were repeated periodically. At 46.6 yrs of age, after years of recurrent sinus infections, the patient underwent sinus surgery at which time she was treated with a 5-day course of oral prednisone at a dosage of 20mg/day. The volumetric indices, V_{tot} and V_{30° , obtained through mathematical modeling of the hill of vision, as elaborated further below, were examined using the screening model in JMP12 to assess magnitude and significance of these variables with regard to correlation with eye, age, and the time of the “Event” of Surgery with concomitant course of oral steroids. Both V_{tot} and V_{30° have been previously reported to have significant correlation with age in normal subjects⁷ and have shown potential use as indicators of progression.⁸ Following the surgery, the patient experienced subjective improvement in both peripheral and central vision. ANOVA confirmed these findings.

Supplementary Figure S3. Graphs of the relationship of visual field indices, V_{tot} and V_{30° , with age and the Event

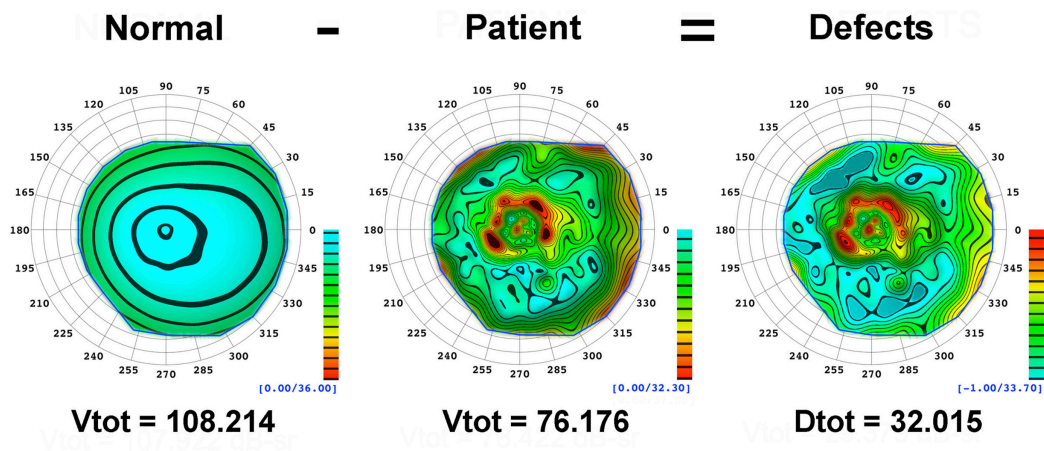


The screening model was used to evaluate for effects of Age, Eye, and Before/After the Event on LogMAR BCVA, V_{tot} , and V_{30° . No significant effect was found of Age on LogMAR BCVA. A significant individual p-value $<.0001$ and simultaneous p-value = $.0006$ was detected for Eye (with greater defect for the right eye) and a significant individual p-value = $.0010$ and a significant simultaneous p-value = $.0140$ was found for the variable Before/After the Event. In both instances, the model created a predictive equation with terms for both before and after sections of the data. LogMAR BCVA detected an effect with Eye (greater for the right eye) and detected the Event. No significant effect of Eye on V_{tot} was found but a significant individual p-value of $.0154$ for Age and a significant individual p-value of $.0185$ for Before/After the Event were found. The simultaneous p-value did not reach significance for either variable. ANOVA indicated no linear effect was present. No effect of Eye was found for V_{30° but a significant individual p-value of $.0053$ for

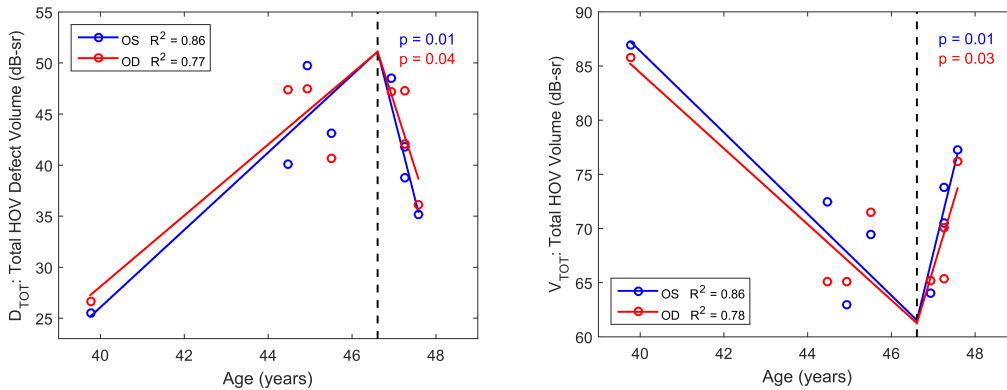
Age, and a marginally insignificant individual p-value of .0510 for Before/After the Event, were found. Both V_{tot} and V_{30° were graphed with a linear and a quadratic fit. The graphs are shown in **Supplementary Figure S3**. Note that the linear fit does not appear to reflect for either eye the Event, which occurred at the time point indicated with the vertical dotted line on the abscissa. The Event is easily visible with the quadratic fit for the right eye and a subtle effect of the Event is visible for V_{30° . Although the quadratic fit appeared to enable recognition of the Event, piecewise linear regression better isolated the relationships before and after the Event. Moreover, piecewise linear regression allowed a statistical p-value to be determined for the overall significance of the fit.

Supplementary Appendix. Analysis of static visual field progression and modeling of the hill of vision and its longitudinal changes.

The figure below shows topographic modeling and volumetric analysis of the hill of vision using age-adjusted normal sensitivity values (left model), sensitivity values from full-field static perimetry of the right eye of the patient at the last test session of the 7.8-year observation period (middle model), and model of the defect space (right model) for this eye. These 3-D models were created using a previously described computer program.⁸ The number below the normal and patient model is the volume of the hill of vision, V_{tot} , which reflects the magnitude and extent of the visual field sensitivity, whereas the volume below the defects model is the volume of defect space, D_{tot} , which reflects how much the patient's data differs from normal. The 3-D defects model is generated using the values obtained after subtraction of the patient's sensitivity value at each test location in the grid from the calculated age-adjusted normal value for that test location. This process results in a hill of defects where positive values indicate the magnitude of the defects. Both indices, V_{tot} and D_{tot} , are in the volumetric unit decibel-steradian (dB-sr). Topographical lines at 2.5 dB intervals and colors help appreciate the level of sensitivity and defects. The left numbers in blue at the bottom of the color scales indicate the base of the model, which for the normal and patient model was at 0 dB. The defects model has a rippled base that extends below the floor of the model in the regions that are a darker teal color. The maximum of these extensions below is -1.0 dB. The right number in blue at the bottom of the color scale indicates the maximum sensitivity level of the entire hill of vision for the normal and patient model and the maximum defect level in the defects model. Note that the maximum sensitivity is 36.00 dB for the normal model, 32.30 dB for the patient model, and 33.70 dB for the defects model.



Piecewise linear regression was utilized to illustrate the rate of change with time. The line graphs below display the changes observed in the volumetric endpoints from the patient hill of vision (V_{tot}) (left) and the hill of defects (D_{tot}) (right) over the period of observation. Loss of sensitivity volume V_{tot} and increase in defects D_{tot} are seen from age 39 to 46.62 yrs., the time of surgery and 5-day course of oral steroids. The p values for OS (blue) and OD (red) indicate the significance of the regression lines after the event. The R^2 values reflect the goodness of fit for the entire 7.8 yrs. of observation.



The piecewise linear regression for the total volume, V_{tot} , for the hill of vision (left) decreased and the defects, D_{tot} , increased in each eye from age 39 years into the early to mid 40's. The patient's vision fluctuated on follow-up visits and appeared to worsen with the occurrence of recurrent bouts of sinusitis after 45 years of age. Use of decongestants and antibiotics provided only temporary relief and were followed by recurrent infections. At 46.62 years of age, sinus surgery was performed in association with a 5-day course of oral steroids. The vision subjectively improved after the surgery with further improvement occurring over the following months. Greater improvements were noted in the peripheral visual field by the patient and these were associated with increased sensitivity on visual field testing. The central region of the visual field underwent more complex changes with portions of the central visual field improved while other central areas showed consolidation of sensitivity losses with deepening, widening, and overall increase in the defects in these regions.

Renderings of longitudinal changes in the 3-D model of the patient hill of visual field sensitivity and hill of defects were created using piecewise linear regression (see online supplemental movies entitled "Lockhart_et_al_HOV_sensitivity.mp4" and "Lockhart_et_al_HOV_defects.mp4"). In the above line plots and their corresponding movies, it can be seen that up to age 46.62 there is progressive loss of visual field sensitivity (V_{tot}) and increase in defects (D_{tot}) both centrally and in the periphery. After the surgery, the sensitivity within the central 10° radius and the peripheral sensitivity of the model increase and the corresponding defects decrease steadily. The pericentral sensitivity between the central 10° and the mid-periphery (out to 20° to 30° eccentricity and along the superior temporal raphe) underwent a different set of changes that included consolidation of losses of sensitivity and deepening and widening of the defects into an absolute partial ring scotoma in each eye.

The improvements in sensitivity following the sinus surgery and steroid therapy offer the possibility that inflammation may play a significant role in the pathogenesis of Bietti crystalline retinal dystrophy. Indeed, there is published evidence that low levels of chronic indolent inflammation are present in the more common inherited retinal degeneration, retinitis

pigmentosa.¹¹ Further studies will be necessary to dissect the impact of chronic inflammation and to determine the role of anti-inflammatory therapies in this inherited retinal degeneration.

References for Supplementary Appendix

1. Weleber RG. The effect of age on human cone and rod Ganzfeld electroretinograms. *Invest Ophthalmol Vis Sci.* 1981;20:392–399.
2. Weleber RG and Eisner A. Retinal Function and Physiological Studies. Chapter 3 in Newsome DA. *Retinal Dystrophies and Degenerations.* Raven Press, New York, 1989, pages 21-69.
3. Weleber RG, Gupta N, Trzuppek KM, Wepner MS, Kurz DE, Milam AH. Electroretinographic and clinicopathologic correlations of retinal dysfunction in infantile neuronal ceroid lipofuscinosis (infantile Batten disease). *Mol Genet Metab.* 2004;83:128–137.
4. Marmor MF, Fulton AB, Holder GE, et al. ISCEV Standard for full-field clinical electroretinography (2008 update). *Doc Ophthalmol.* 2009;118:69–77.
5. Machida S. Clinical applications of the Photopic Negative Response to Optic Nerve and Retinal Diseases. *Journal of Ophthalmology* 2012, Article ID 397178, 11 pages doi:10.1155/2012/39178
6. Viswanathan S, Frishman LJ, Robson JG, Walters JW. The Photopic Negative Response of the Flash Electroretinogram in Primary Open Angle Glaucoma. *Invest Ophthalmol Vis Sci.* 2001; 42:514-522.
7. Weleber RG, Pennesi ME, Wilson DJ, et al. Results at 2 years after Gene Therapy for RPE65-deficient Leber Congenital Amaurosis and Severe Early-Childhood Onset Retinal Dystrophy. *Ophthalmology.* 2016;123:1606-1620. Supplemental materials available at the following website: [http://www.aaojournal.org/article/S0161-6420\(16\)00339-0/abstract](http://www.aaojournal.org/article/S0161-6420(16)00339-0/abstract)
8. Weleber RG, Smith TB, Peters D, et al. VFMA: Topographic Analysis of Sensitivity Data From Full-Field Static Perimetry. *Transl Vis Sci Technol* 2015;4(2):14 doi: 10.1167/tvst.4.2.14.
9. Gardiner SK, Demirel S, Johnson CA, Swanson WH. Assessment of linear-scale indices in perimetry in terms of progression in early glaucoma. *Vision Res.* 2011; 51(16): 1801-1810.
10. Jones BW, Watt CB, Frederick JML, Baehr W, Chen C-K,, Levine EM, Milam AH, LaVail M, Marc RE. Retinal Remodeling Triggered by Photoreceptor Degenerations. *The Journal of Comparative Neurology.* 2003 464: 1-16.
11. Yoshida N, Ikeda, Y, Notomi, S, et al. Clinical evidence of sustained chronic inflammatory reaction in retinitis pigmentosa. *Ophthalmol* 2012;120(1):100-5 doi: 10.1016/j.ophtha.2012.07.008